

Dynamics of anchored polymers under an oscillating force

A. K Chattopadhyay¹, D. Marenduzzo²

¹ *Universita' degli Studi di Padova, Dipartimento di Fisica "G. Galilei", via Marzolo 8, 35131 Padova, Italy*

² *SUPA, School of Physics, University of Edinburgh, Edinburgh EH9 3JZ, UK*

Using 3D Monte Carlo kinetic simulations and analytical theory, we analyze the dynamics of a series of polymers of varying stiffness pinned or grafted at both ends and subjected to an oscillatory forcing at an intermediate point. We find a crossover from a periodic limit cycle behavior to a more complex aperiodic dynamics as the polymer gets 'stiffer', suggesting the presence of hysteresis and memory. An analytical evaluation of the Lyapunov exponent leads to the conjecture that the hysteresis in stiff polymers might be a signature of mild chaos.

PACS numbers: 36.20.Ey, 87.15.La, 64.60.Ht, 87.15.He

Recent times have witnessed a remarkable outburst in the development and use of single molecule techniques [1, 2]. These have now made it possible to grab a single molecule with atomic force microscopes (AFMs), soft micro-needles, laser tweezers etc. and to apply a local force of a prescribed shape ideally at any section of the polymer under scrutiny (though so far this has mostly been done at one of the polymer ends). While these experiments are of interest per se, as they allow precise measurements of elastic properties (such as persistence length, bending and stretching modulus) of bio- and artificial polymers, they may also shed some light on several in vivo situations in which cellular machineries or protein complexes exert a localized controlled force on segments of a bio-polymer such as DNA or another biofilament. A widely accepted example of this is found in DNA unzipping during replication, in which DNA helicases bind at the two ends of an "eye" (or replication bubble) and unwind the double helix locally [3, 4]. Other suggestive examples occur during DNA transcription, when RNA polymerases may apply a significant local force to reel in a gene, in order to transcribe it [5], or in cytoskeletal dynamics, as motor proteins continuously push and pull actin fibers and microtubules [3].

With some notable exceptions [6, 7], theory and experiments have most often focused on an equilibrium description, aimed e.g. at analyzing the restoring force versus end-to-end distance. While this is definitely of interest and works remarkably well in e.g. fitting the force-elongation curves for double-stranded (ds) DNA via the worm-like chain model [2], there remains a host of interesting questions concerning the dynamics of a single polymer which can provide a more convincing agreement between theory and experiments [8].

Here we suggest a possible set-up for a single molecule experiment whose dynamics is at the same time non-trivial and amenable to a detailed comparison with theoretical predictions. We consider a polymer of variable stiffness anchored at both its ends, and subjected to a periodic oscillatory force at an interior point. By monitoring the three-dimensional real space time evolution of the polymer chunk which is under tension by means of dynamic Monte-Carlo simulations, we predict a crossover from a periodic linear cycle in the position-force plane, typically observed for very flexible chains, to an aperiodic behavior for stiffer polymers. The shape of this orbit

depends on the magnitude and periodicity of the forcing. An analytical treatment of the close-to-equilibrium tip dynamics of a two-dimensional polymer grafted at one end, allows us to prove that (at least in that case) there is a positive Lyapunov exponent in the semi-flexible limit. The different dynamical states we predict may be checked via present day experiments using laser tweezers in which the point of application of the force can be accurately controlled. This would yield time series of the data analogous to the ones we compute. The polymer needs to be perturbed with a frequency larger than or comparable to its inverse relaxation time in order to observe the phenomena we predict. Given typical relaxation times of bio-polymers, ideal candidate systems to verify our predictions *might be long dsDNA molecules or actin or amyloid fibers (whose relaxation times ranges from ms to s, see the discussion at the end)* [1].

We first consider the full 3-dimensional dynamics of a (strictly inextensible) semi-flexible and self-avoiding polymer (of variable stiffness) subject to a time dependent force $\vec{f}(t)$ applied at the j -th bead of the chain, with $j = sN$ with $0 < s < 1$ (the chain is constituted by N beads of diameter $0.9a$ joined by $N - 1$ links of length a , in what follows a is set equal to 1). We follow the time evolution of the polymer via three dimensional dynamic Monte Carlo (3DdMC) simulations involving the kink-jump algorithm [9], which are qualitatively analogous to molecular dynamics. One Monte-Carlo step (MCS) corresponds to a series of N attempted kink-jump moves. This method has recently been successfully used in a number of contexts [10, 11], both on and off lattice. Although it does not allow a direct mapping to physical times, and it disregards hydrodynamic interactions between beads, in the present case it is useful as it allows an exact handling of the inextensibility constraint, as there is no need to introduce soft springs between monomers. The Hamiltonian, \mathcal{H} , describing the single molecule set-up we are interested in is then:

$$\mathcal{H} = K_b \sum_{i=1}^{N-2} \vec{t}_i \cdot \vec{t}_{i+1} + \vec{f}(t) \cdot \vec{r}_{sN} \quad (1)$$

where $K_b \equiv L_p k_B T$ is the bending rigidity (L_p , k_B and T are respectively the persistence length, Boltzmann constant and temperature) and \vec{t}_i denotes the i -th link ($1 \leq i < N$). Results are primarily reported for pinned boundary conditions. This

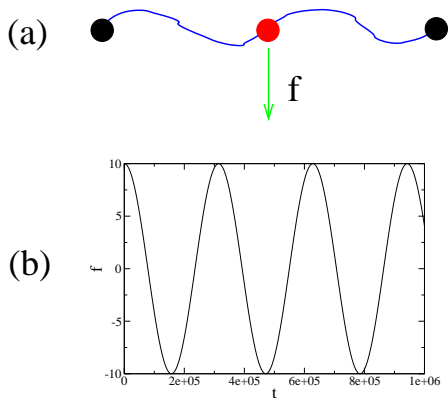


FIG. 1: Set-up of our calculation. A semi-flexible chain pinned at both ends (a) is acted upon by an oscillating force (b) on the mid-point, or at a generic point between its extremities.

means that the first and last beads are constrained to stay at $(0, 0, 0)$ and $(d, 0, 0)$, with $d < L \equiv Na = N$. For selected cases, we considered polymers grafted at (i) one end ($i = 1$), and (ii) both ends. In these cases the first and last link were constrained to lie along the x direction as well. Typical values for other parameters were $L = 100$, $d/L = 0.6$, and L_p/L between 0 and 0.2 (we also confirmed our results for smaller values of d/L). The periodic force along the z direction is given by $\vec{f}(t) = \hat{z}A \cos(2\pi\omega t)$, where A is the amplitude of the perturbation (typically $10 k_B T/a$) and $\omega \equiv 1/\tau$ its inverse period. Fig. 1 shows the set-up considered.

In what follows, time is measured in MCSs, as usual in related calculations. To relate this to physical quantities, for each of the case studied we will also report estimates for the polymer relaxation time, τ_r . We also note that the 3D MC algorithm we use works at a fixed temperature T , while quantities such as bead diffusion and friction cannot be inputted and have to be calculated *a posteriori*.

Figs. 2 and 3 show the dynamic trajectories in the $(z_{L/2}(t) \equiv z(t), f(t))$ plane for a flexible (Fig. 2, variable ω) and a semi-flexible (Fig. 3, L_p/L from 0 to 0.1) polymer chain respectively, fixed at both ends. The flexible polymer parameters may be mapped onto those of a polyethylene molecule of thickness ~ 0.5 nm and contour length 50 nm, while the semi-flexible polymer with $L_p/L = 0.1$ may represent e.g. a DNA molecule of $0.5 \mu\text{m}$ contour length in a $0.1 M$ NaCl solution (which is close to physiological concentration), for which its effective thickness is 5 nm [12].

We begin with the flexible case. If we were in quasi-equilibrium, so that at any time the position of the mid point along z were equal to the equilibrium ensemble averaged over a polymer subject to a force $f(t)$ (this requires $\omega \rightarrow 0$), the dynamic trajectory in the (z, f) plane would be confined to the one-dimensional curve defined by $z(t) = \frac{\partial \log(Z(\beta f, d))}{\partial \beta f}$, where Z is the partition function of the system (which depends on d as well when both ends are anchored). In most cases the form of $z(t)$ cannot be found explicitly.

Fig. 2a shows that if $\tau \gg \tau_r$, then quasi-equilibrium is

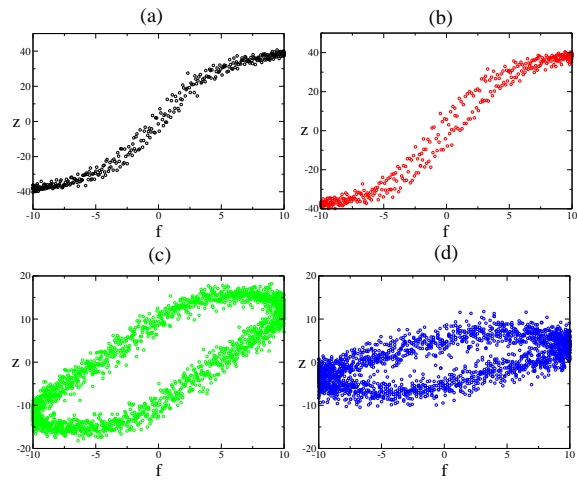


FIG. 2: Plot of $(z(t), f(t))$ for a flexible polymer with $1/\omega$ equal to (a) 20000, (b) 1000, (c) 500 and (d) 250 (in MCSs). τ_r was estimated to be 2500 MCSs. $z(t)$ and $f(t)$ are in units of a and $k_B T/a$ respectively.

recovered. In Figs. 2b and 2c non-equilibrium effects creep in, and the quasi-equilibrium line is substituted by a hysteresis (2b) or a limit cycle (2c). This crossover is due to the fact that the chain can no longer equilibrate at all times during the force ramping cycle, because now $\tau \sim \tau_r$. As a result, the mid-point position is sampled only on a portion of the phase space, which yields an under(over)-estimate of its value in the forward (backward) force scan, hence hysteresis shows up. Equivalently, hysteresis can be interpreted as due to the fact that disturbances along the chain now decay on a time scale which is not any more much shorter than the forcing period (their velocity is finite). If ω is further increased (Fig. 2d), the trajectory followed by the limit cycle tilts toward the f -axis, so that keeping the amplitude of the perturbation fixed, the elongation of the mid-point along the z -axis is smaller.

The crossover between quasi-equilibrium and limit cycle behavior should be observed in a flexible polymer with a short persistence length. (*Suitable candidates for an experiment would be long dsDNA's, with $L = 50 \mu\text{m}$ or more, hence essentially flexible polymers with $\tau_r > 1$ s.*) A stiffer polymer, such as a relatively short dsDNA or an actin fiber, enhances the hysteresis and eventually the polymer relaxation time becomes too large with respect to the period of the oscillations. Under such circumstances, we no longer observe a (noisy) limit cycle but the trajectories, representing the motion of the polymer mid-point, now fill the space in the (z, f) plane.

Fig. 3 shows the crossover between these two different regimes. The limit cycle behavior typical of the flexible chain changes over to the space filling trajectories for stiffer semi-flexible polymers as we increase L_p/L . This space filling trajectory can be thought of as the superposition of several limit cycles each of which only spans a limited range in z during a force cycle (forward and backward scan). This crossover closely resembles what happens in a Poincaré section in sys-

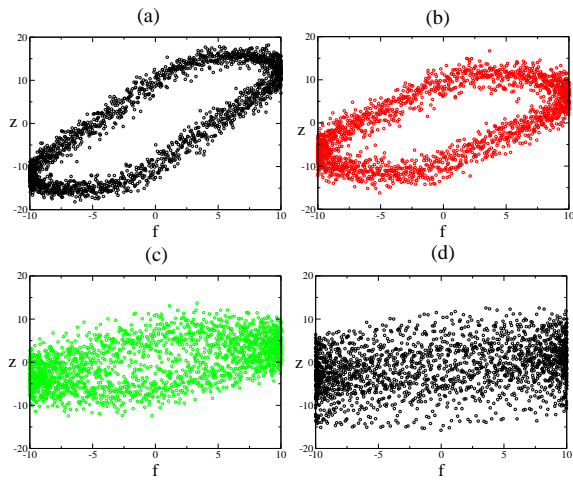


FIG. 3: Plot of $(z(t), f(t))$ for a polymer with $L = 100a$, $d/L = 0.6$, and with variable stiffness (respectively $L_p/L = 0$ (a), $L_p/L = 0.02$ (b), $L_p/L = 0.05$ (c) and $L_p/L = 0.1$ (d)). x labels the time dependent position of the mid-point along the chain (at $s = L/2$). τ was 500 MCSs, while τ_r was estimated to be (a) 2500, (b) 13500, (c) 67500 and (d) 110000 (in units of MCSs [15]). $z(t)$ and $f(t)$ are in units of a and $k_B T/a$ respectively.

tems crossing over from a limit cycle behavior to chaotic dynamics (see e.g. [13]). As time progresses, the instantaneous limit cycle at the mid-point is visiting drifts (upwards and downwards along the z axis in Fig. 3) in a random walk fashion, and this gives the aperiodicity to the dynamics.

To assess the robustness of our results, we also performed calculations with different boundary conditions, namely with polymers grafted at one or both ends. In all cases a crossover was found upon increasing L_p at a fixed L . The crossover value L_p^*/L is smaller with grafted boundary conditions (it is “easier” to get into the aperiodic regime there); while it only weakly depends on chain length over the values considered (L between 50 and 200 a for pinned boundary conditions). We have attempted to qualitatively estimate the effect of hydrodynamic interactions, by performing simulations of the same system described by the potential in Eq. (1) with the stochastic rotation model [14] (this requires the introduction of soft non-linear “FENE” springs between monomers). While the crossover between a limit cycle to an aperiodic regime is still observed, our simulations suggest that the crossover occurs for larger L_p and ω than in the 3D MC simulations (the aperiodic region in the dynamic phase diagram shrinks due to hydrodynamics). Details will be presented elsewhere.

It is instructive to compare our simulations with a semi-analytical treatment of the tip dynamics, in order to physically explain the striking onset of a “chaotic” behaviour in the dynamics of a single semi-flexible polymer. To this aim, for concreteness it is helpful to focus on the case of a semi-flexible polymer grafted along the x direction and subject to an oscillating transverse force along the z direction perturbation at its end, and to restrict to a 2-dimensional analysis. This is because in this case several semi-analytic results for

the equilibrium properties of the polymer in the unforced case are now known from [16] (our simulations *do* appear to show the same physics for grafted chains as well, at least in $d = 3$, see above.) We then couple these semi-analytical results to the theoretical technique reported in [17] to derive the Lyapunov exponent for grafted polymers.

On general grounds we may write the following equation, valid for close-to-equilibrium tip dynamics:

$$\dot{z}(t) = -\Gamma \frac{\delta}{\delta z(t)} [k_B T \log P(z)] + f(t) + \eta(t) \quad (2)$$

$$P(z) = \frac{L_p \sqrt{3}}{\pi L^2} \int_{-\infty}^{\infty} d\theta \exp\left\{-\frac{L_p \theta^2}{2L}\right\} \exp\left\{-\frac{6L_p [z - \sin \theta L]^2}{L^3}\right\}, \quad (3)$$

where δ denotes a functional derivative, the form of the transverse tip probability distribution $P(z)$ (whose logarithm defines $-\mathcal{F}(z)/k_B T$, $\mathcal{F}(z)$ being the free energy which governs the tip dynamics) is borrowed from [16], Γ is a suitable relaxation time and η is a random noise whose 2-point correlation is $\langle \eta(t)\eta(t') \rangle = 2D\delta(t-t')$ ($D > 0$ gives the strength of noise). From now on we set $\Gamma = 1$ which amounts to a rescaling of time (and hence of the Lyapunov exponent).

The dynamics originating from Eq. 2 can be studied with the methods of [17] which lead to the following estimate for the largest Lyapunov exponent of the system, λ :

$$\lambda = \frac{1}{2} \int d\tau' \langle \zeta(\tau') \zeta(\tau + \tau') \rangle \cos 2\omega\tau' \quad (4)$$

where we have defined $\zeta(t) = \mathcal{F}''(z)$ [17].

For a determination of the Lyapunov exponent via Eq. 4, we need to resort to a numerical solution for the tip dynamics as per Eq. 2. However it is instructive to find an approximate semi-analytical estimate. To this purpose, we have numerically evaluated $\mathcal{F}(z)$ and fitted it to the function $f(z) \equiv f_0 + a(z/L)^4 - b(z/L)^2$, with f_0 an irrelevant constant. $f(z)$ is a double well for $a, b > 0$. At this point we can directly use the results in [17] to find the following approximation for the largest Lyapunov exponent:

$$\lambda = \frac{9}{8} \left(1 - \frac{aD}{b^2}\right)^2 \frac{\sqrt{b} \left(1 + \frac{b}{4a}\right)}{\left[1 + b \left(1 + \frac{b}{4a}\right)^2\right]}. \quad (5)$$

where $b(L_p/L)$ and $a(L_p/L)$ are to be found numerically. The value of λ obtained through Eq. 5 is approximate and thus e.g. it only vanishes for $L_p/L < 0.25$, while a numerical estimate shows that $\lambda=0$ for $L_p < xL$ with $x \sim 0.4$.

Fig. 4 shows the analytical approximation and numerical estimate for the Lyapunov exponent of a grafted polymer. Both show that the Lyapunov exponent increases with stiffness in the semiflexible polymer regime, as found by the simulations. Interestingly the semi-analytical treatment predicts that λ should also vanish for L_p/L large. Our approximation also highlights the physical origin of the onset of chaos

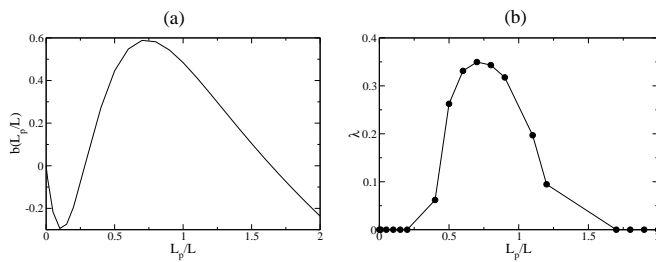


FIG. 4: Plot of (a) b (whose sign determines whether the effective potential is a single or a double well), and (b) λ , as a function of L_p/L for $L = 100a$, and $D = 0.1$, using Eq. (6).

in semi-flexible polymers of intermediate stiffness in the numerical simulations. As shown in [16] and as is apparent from Eq. 2 and its approximation, in 2D the distribution probability of the tip position of a grafted semi-flexible polymer is bimodal for intermediate stiffness. Hence the effective free energy governing the tip dynamics (in the close-to-equilibrium regime) is perhaps the simplest paradigm leading to chaotic motion (in the weak damping and deterministic limit this is the well known Duffing oscillator [13]). Our simulations are in 3D, and include pinned as well as grafted boundary conditions, but it is reasonable to postulate that the weakly chaotic regime we observe is given by the same physics leading to chaos in the above calculation. (Ref. [16] suggests a slow relaxation of transverse tip fluctuations so a dynamic study like ours may introduce additional local minima thereby making the chaotic signature of the dynamics more pronounced than in the close-to-equilibrium calculation above.)

Is the crossover from limit cycle to weak chaos observable with a state-of-the-art single molecule experiment? To assess that, we note that, for this to be possible, a controlled force experiment needs to be performed, with the force cycling between $-A$ and A , with a frequency increased up to a value $> \tau_r^{-1}$. E.g. an AFM force-clamp needs $\sim ms$ feedback to work [18], while it can provide up to $\sim 100 pN$ of force (a laser tweezer would provide more stringent constraints). τ_r can be accurately estimated via the modified Rouse theory reported in [19] (Eq. (5) of that work). For a short dsDNA ($L \sim 0.5 \mu m$, $a = 5 nm$, $L_p = 50 nm$), an actin fiber ($L \sim 2 \mu m$, $L_p \sim 17 \mu m$, $a \sim 5 nm$), and an insulin amyloid fiber ($L \sim 10 \mu m$, $L_p \sim 7 \mu m$, $a \sim 5 nm$ [20]), in an aqueous solution, $\tau_r \sim 0.2 ms$, $1 s$ and $10 s$ respectively. Additional simulations suggest that $A \sim tens of pN$ suffices to enter the “chaotic” regime for actin and insulin fibers as well. Therefore we suggest that our predictions may be testable with actin or insulin fibers in an AFM force-clamp (the insulin fiber experiment may possibly be also doable with laser tweezers).

In conclusion, we have studied the dynamics of a semiflexible polymer grafted or pinned at its ends, and subject to a periodic forcing acting on one of its beads. The time series of the process retain strong signatures of non-equilibrium effects. In particular, we observe a crossover between a limit cycle behavior, which reflects the hysteresis inherent in the process, to

another behavior, with features akin to (weak) chaos. A semi-analytical approximation in the quasi-static limit allows us to estimate the largest Lyapunov exponents of a grafted semi-flexible polymer in two dimensions, which suggests that the observed chaotic dynamics, at least in part, originates from non-trivial features in the tip distribution probabilities. More work is now needed to clearly separate thermodynamic and kinetic effects in the dynamic crossover we find. We hope our studies will stimulate experiments to test the existence of this crossover in the kinetics of a single polymer.

We thank O. E. Akman for very useful discussions. AKC acknowledges support from the Marie Curie Foundation, Incoming International Fellowship MIFI-CT-2005-008608.

-
- [1] C. Bustamante, J. C. Macosko, G. J. L. Wuite, *Nat. Rev. Mol. Cell Bio.* **1**, 130 (2000); U. Bockelmann, *Curr. Opin. Struct. Biol.* **14**, 368 (2004); D. E. Smith, H. P. Babcock, S. Chu, *Science* **283**, 1724 (1999).
 - [2] J. F. Marko, E. D. Siggia, *Macromolecules* **28**, 8759 (1995).
 - [3] B. Alberts *et al*, *Molecular biology of the cell*, 4th edition, Garland Science (2003).
 - [4] S. M. Bhattacharjee, F. Seno, *J. Phys. A* **36**, L181 (2003); R. Kapri, S. M. Bhattacharjee, F. Seno, *Phys. Rev. Lett.* **93**, 248102(2004).
 - [5] P. R. Cook, *Science* **284**, 1790 (1999).
 - [6] G. Altan-Bonnet, A. Libchaber, O. Krichevsky, *Phys. Rev. Lett.* **90**, 138101 (2003); R. Shusterman *et al.*, *Phys. Rev. Lett.* **92**, 048303 (2004); A. Meller, L. Nivon, D. Branton, *Phys. Rev. Lett.* **86**, 3435 (2001); S. E. Henrickson *et al.*, *Phys. Rev. Lett.* **85**, 3057 (2000). K. Pant, R. L. Karpel, M. C. Williams, *J Mol Biol* **327**, 571 (2003).
 - [7] A. V. Chechkin *et al.*, *Phys. Rev. E* **67**, 010102(R) (2003), D. K. Lubensky, D. R. Nelson, *Biophys. J.* **77**, 1824 (1999); T. Ambjörnsson, R. Metzler, *Phys. Rev. E* **72**, 030901(R).
 - [8] M. Doi, S. F. Edwards *The theory of polymer dynamics*, Clarendon Press (1988).
 - [9] A. Baumgartner, K. Binder, *J. Chem. Phys.* **71**, 2541 (1979).
 - [10] M. Muthukumar, *Phys. Rev. Lett.* **86**, 3188 (2001).
 - [11] D. Marenduzzo *et al.*, *Phys. Rev. Lett.* **88**, 028102 (2002); N. J. Burroughs, and D. Marenduzzo, *J. Chem. Phys.* **123**, 174908 (2005).
 - [12] V. V. Rybenkov, N. R. Cozzarelli, and A. V. Vologodski, *Proc. Natl. Acad. Sci. USA* **90**, 5307 (1993).
 - [13] S. H. Strogatz, *Nonlinear Dynamics and Chaos*, Addison-Wesley (1995).
 - [14] A. Malevanets, R. Kapral, *J. Chem. Phys.* **110**, 8605 (1999); I. Ali, D. Marenduzzo, J. M. Yeomans, *Phys. Rev. Lett.* **96**, 208102 (2006).
 - [15] One MCS may be mapped to $\sim 2 ns$ in a water-like solvent.
 - [16] G. Lattanzi, T. Munk and E. Frey, *Phys. Rev. E* **69**, 021801 (2004); P. Benetatos, T. Munk, E. Frey, *Phys. Rev. E* **72**, 030801(R) (2005).
 - [17] S. Datta, J. K. Bhattacharjee, *J. Phys. A* **34**, L603 (2001).
 - [18] M. Schlierf, H. Li, J. M. Fernandez, *Proc. Natl. Acad. Sci USA* **101**, 7299 (2004).
 - [19] J.-C. Meiners, S.R. Quake, *Phys. Rev. Lett.* **84**, 5014 (2000).
 - [20] J. F. Smith *et al.*, *Proc. Natl. Acad. Sci. USA* **103**, 15806 (2006).